

Final Report

DOE DE-FG02-04ER46126
University of Massachusetts

Nanoparticle Assemblies at Fluid Interfaces

Thomas P. Russell

Reporting Period:

3/15/04-3/14/14

Patents

M. Cui, T.P. Russell and T. Emrick, "Stabilizing Liquids Drops of Arbitrary Shape by the Interfacial Jamming of Nanoparticles", Patent Application, Sept. 24, 2014.

Publications

1. E. Glogowski, J.B. He, T.P. Russell and T. Emrick, "Mixed Monolayer Coverage on Gold Nanoparticles for Interfacial Stabilization of Immiscible Fluids," *Chemical Communications*(32), 4050-4052 (2005).
2. K.A. Leach, S. Gupta, M.D. Dickey, C.G. Willson and T.P. Russell, "Electric Field and Dewetting Induced Hierarchical Structure Formation in Polymer/Polymer/Air Trilayers," *Chaos* 15(4), Art. No. 047506 (2005).
3. K.A. Leach, Z. Lin and T.P. Russell, "Early Stages in the Growth of Electric Field-Induced Surface Fluctuations," *Macromolecules* 38, 4868-4873 (2005).
4. Y. Lin, A. Böker, H. Skaff, D. Cookson, A.D. Dinsmore, T. Emrick and T.P. Russell, "Nanoparticle Assembly at Fluid Interfaces: Structure and Dynamics," *Langmuir* 21, 191-196 (2005).
5. Y. Lin, A. Böker, K. Sill, H. Xiang, C. Abetz, J. Wang, T. Emrick, A. Balazs and T. P. Russell, "A Self-Directed Self Assembly of Nanoparticles and Block Copolymers," *Nature* 434, 55-59 (2005).
6. J.T. Russell, Y. Lin, A. Boeker, L. Su, P. Carl, H. Zentl, J. He, K. Sill, R. Tangirala, T. Emrick, K. Littrell, P. Thiyagarajan, D. Cookson, A. Fery, Q. Wang and T.P. Russell, "Self-Assembly and Cross-Linking of Bionanoparticles at Liquid-Liquid Interfaces," *Angew. Chem. Int. Ed.* 44, 2-8 (2005).
7. H. Skaff, Y. Lin, R. Tangirala, K. Breitenkamp, A. Boeker, T.P. Russell and T. Emrick, "Crosslinked Capsules of Quantum Dots by Interfacial Assembly and Ligand Crosslinking," *Adv. Mater.* 17, 2082-2086 (2005).
8. Q. Zhang, T. Xu, D. Butterfield, M.J. Misner, D.Y. Ryu, T. Emrick and T.P. Russell, "Controlled Placement of CdSe Nanoparticles in Diblock Copolymer Templates by Electrophoretic Deposition," *Nano Letters* 5(2), 357-361 (2005).
9. A. C. Balazs, T.S. Emrick and T.P. Russell, "Nanoparticle Polymer Composites: Where Two Small Worlds Meet," *Science* 314, 1107-1110 (2006).

10. E. Glogowski, R. Tangirala, T.P. Russell and T. Emrick, "Functionalization of Nanoparticles for Dispersion in Polymers and Assembly in Fluids," *Journal of Polymer Science, Part A: Polymer Chemistry* 44(17), 5076 (2006).
11. S. Gupta, Q. Zhang, T. Emrick, A.C. Balazs and T.P. Russell, "Entropy-Driven Segregation of Nanoparticles to Cracks in Multilayered Composite Polymer Structures," *Nature Mats.* 5(3), 229-233 (2006).
12. S. Gupta, Q. Zhang, T. Emrick and T.P. Russell, "Self-Corralling Nanorods under an Applied Electric Field," *Nano Letters* 6(9), 2066 (2006).
13. A. Böker, J. He, T.S. Emrick and T.P. Russell, "Self-Assembly of Nanoparticles at Interfaces," *Soft Matter* 3, 1231-1248 (2007).
14. E. Glogowski, R. Tangirala, J. He, T.P. Russell and T. Emrick, "Microcapsules of Pegylated Gold Nanoparticles Prepared by Fluid-Fluid Interfacial Assembly," *Nano Letters* 7, 389-393 (2007).
15. J. He, J.-Y. Wang, R. Tangirala, D. Shin, X. Li, J. Wang and T.P. Russell, "On the influence of ion incorporation in thin films of block copolymers," *Advanced Materials* 19, 4370-4374 (2007).
16. J. He, R. Tangirala, A. Boeker, X. Li, J. Wang, T. Emrick and T.P. Russell, "Self-Assembly of Nanoparticle-Copolymer Mixtures: A Kinetic Point of View," *Adv. Mater.* 19, 381-385 (2007).
17. J. He, Q. Zhang, S. Gupta, T. Emrick, T.P. Russell and P. Thiyagarajan, "Drying Droplets: A Window into the Behavior of Nanorods at Interfaces," *Small* 3, 1214-1217 (2007).
18. S. Kutuzov, J. He, R. Tangirala, T. Emrick, T.P. Russell and A. Boeker, "Kinetics on the Nanoparticle Self-Assembly at Liquid-Liquid Interfaces," *Phys. Chem. Chem. Phys.* 9, 6351-6358 (2007).
19. T. Li, Z. Niu, T. Emrick, T.P. Russell and Q. Wang, "Raspberry-Like Core-Shell Nanocomposite from Hierarchical Assembly of Virus and Polymer," *Virus Nanotechnology* DOI: 10.1002/anie.2007 (2007).
20. R. Tangirala, R. Revanur, T.P. Russell and T.S. Emrick, "Sizing Nanoparticle-Covered Droplets by Extrusion through Track-Etch Membranes," *Langmuir* 23(3), 965-969 (2007).
21. T. Li, Z.W. Niu, T. Emrick, T.P. Russell, Q. Wang, "Core/Shell Biocomposites from the Hierarchical Assembly of Bionanoparticles and Polymer," *Small* 4(10), 1624-1629 (October 2008).
22. Q.F. Li, J.B. He, E. Glogowski, X.F. Li, J. Wang, T. Emrick, T.P. Russell, "Responsive Assemblies: Gold nanoparticles with Mixed Ligands in Microphase Separated Block Copolymers," *Advanced Materials* 20(8), 1462-+ (April 2008).
23. M.A. Bruckman, G. Kaur, L.A. Lee, F. Xie, J. Sepulveda, R. Breitenkamp, X. Zhang, M. Joralemon, T.P. Russell, T. Emrick and Q. Wang, "Surface Modification of Tobacco Mosaic Virus with "Click" Chemistry", *Chembiochem*, 9(4), 519-523, (March 2008).
24. Q.L. Zhang, A. Cirpan, T.P. Russell and T. Emrick, "Donor-Acceptor Poly(thiophene-block-perylene diimide) Copolymers: Synthesis and Solar Cell Fabrication," *Macromolecules* 42(4), 1079-1082 (February 2009).
25. J.B. He, Z.W. Niu, R. Tangirala, J.Y. Wan, X.Y. Wei, G. Kaur, Q. Wang, G. Jutz, A. Boeker, B. Lee, S.V. Pingali, P. Thiyagarajan, T. Emrick and T.P. Russell,

- "Self-Assembly of Tobacco Mosaic Virus at Oil/Water Interfaces," *Langmuir* 25(9), 4979-4987 (May 2009).
26. G. Kaur, J.B. He, J. Xu, S.V. Pingali, G. Jutz, A. Boeker, Z.W. Niu, T. Li, D. Rawlinson, T. Emrick, B. Lee, P. Thiyagarajan, T.P. Russell and Q. Wang, "Interfacial Assembly of Turnip Yellow Mosaic Virus Nanoparticles," *Langmuir* 25(9), 5168-5176 (May 2009).
 27. Z.W. Niu, S. Kabisatpathy, J.B. He, L.A. Lee, J.H. Rong, L. Yang, G. Sikha, B.N. Popov, T.S. Emrick, T.P. Russell and Q. Wang, "Synthesis and Characterization of Bionanoparticle-Silica Composites and Mesoporous Silica with Large Pores," *Nano Research* 2(6), 474-483 (June 2009).
 28. K. Du, C.R. Knutson, E. Glogowski, K.D. McCarthy, R. Shenhar, V.M. Rotello, M.T. Tuominen, T. Emrick, T.P. Russell and A.D. Dinsmore, "Self-Assembled Electrical Contact to Nanoparticles Using Metallic Droplets", *Small*, 5(17), 1974-1977 (September 2009).
 29. R. Tangirala, Y.X. Hu, M. Joralemon, Q.L. Zhang, J.B. He, T.P. Russell and T. Emrick, "Connecting Quantum Dots and Bionanoparticles in Hybrid Nanoscale Ultra-Thin Films," *Soft Matter* 5(5), 1048-1054 (2009).
 30. G.V. Kolmakov, R. Revanur, R. Tangirala, T. Emrick, T.P. Russell, A.J. Crosby and A.C. Balazs, "Using Nanoparticle-filled Microcapsules for Site-specific Healing of Damaged Substrates: Creating a 'Repair-and-Go' System", *ACS Nano* 4(2), 1115-1123 (2010).
 31. K. Du, E. Glogowski, T. Emrick, T.P. Russell and A. Dinsmore, "Adsorption Energy of Nano- and Microparticles at Liquid-Liquid Interfaces", *Langmuir* 26 (15), 12518-12522, (2010).
 32. L. Li, C. Miesch, P.K. Sudeep, A.C. Balazs, T. Emrick, T.P. Russell, and R. C. Hayward, "Kinetically Trapped Co-Continuous Polymer Morphologies through Intraphase Gelation of Nanoparticles," *Nano Letters*, 11(5): 1997-2003, (2011).
 33. C. Miesch, I. Kosif, E. Lee, J.K. Kim, T.P. Russell, R.C. Hayward and T. Emrick, "Nanoparticle-Stabilized Double Emulsions and Compressed Droplets," *Angewandte Chemie-International Edition*, 51(1): 145-149, (2012).
 34. X. Wei, W. Gu, W. Chen, X. Shen, F. Liu, J.W. Strzalka, Z. Jiang and T.P. Russell, "Disorder-to-Order Transitions Induced by Alkyne/Azide Click Chemistry in Diblock Copolymer Thin Films," *Soft Matter*, 8(19): 5273-5282, (2012).
 35. K. Kratz, A. Narasimhan, R. Tangirala, S. Moon, R. Revanur, S. Kundu, H.S. Kim, A.J. Crosby, T.P. Russell, T. Emrick, G. Kolmakov and A.C. Balazs, "Probing and Repairing Damaged Surfaces with Nanoparticle-Containing Microcapsules," *Nature Nanotechnology*, 7(2): 87-90, (2012).
 36. X. Li, S.W. Shen, R.C. Hong, R.C. Hayward and T.P. Russell, "Fabrication of Co-continuous Nanostructured and Porous Polymer Membranes through Spinodal Decomposition of Homopolymer/Random Copolymer Blends," *Angewandte Chemie*, 51(17), 4089-4094, (2012).
 37. G.V. Kolmakov, T.S. Emrick, T.P. Russell, A.J. Crosby and A.C. Balazs, "Design of a Repair-and-Go System for Site-Specific Healing at the Nanoscale," V. Amendola and M. Meneghetti editors, CRC Press, (2012).

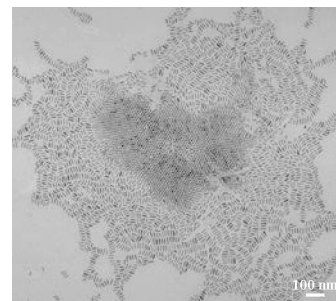
38. C. Miesch, I. Kosif, E. Lee, J.-K. Kim, T.P. Russell, R.C. Hayward and T. Emrick, "Nanoparticle-Stabilized Double Emulsions and Compressed Droplets," *Angewandte Chemie – International Edition*, 51(1), 145-149, (2012).
39. I. Kosif, M. Cui, T.P. Russell and T.S. Emrick, "Triggered in situ Disruption and Inversion of Nanoparticle-Stabilized Droplets," *Angewandte Chemie*, DOI: 10.1002/anie.201302112, (2013).
40. M. Cui, T. Emrick and T.P. Russell, "Stabilizing Liquid Drops in Nonequilibrium Shapes by the Interfacial Jamming of Nanoparticles," *Science* 342(6157), 460-463, DOI: 10.1126/science.1242852, (October 25, 2013).
41. P. Kim, E. David, L. Raboin, A.E. Ribbe, T.P. Russell and David A. Hoagland, "Ionic Liquids as Flootation Media for Cryo-Ultramicrotomy of Soft Polymeric Materials," *Microscopy and Microanalysis* 19(6), 1554-1557, (December 2013).
42. Z. Sun, T. Feng and T.P. Russell, "Assembly of Graphene Oxide at Water/Oil Interfaces: Tessellated Nanotiles," *Langmuir* 29(44), 13407-13413, (November 2013).
43. J. Bae, T.P. Russell, and R.C. Hayward, "Osmotically Driven Formation of Double Emulsions Stabilized by Amphiphilic Block Copolymers," *Angewandte Chemie-International Edition* 53(31), 8240-8245, DOI: 10.1002/anie.201405229, (July 2014).
44. T. Feng, D.A. Hoagland, and T.P. Russell, "Assembly of Acid-Functionalized Single-Walled Carbon Nanotubes at Oil/Water Interfaces," *Langmuir* 30(4), 1072-1079, DOI: 10.1012/la404543s, (January 2014).

Accomplishments

Interfacial Behavior of CdSe Nanorods: Unlike isotropic colloidal particles, nanorods at interfaces show interesting responses due to their shape. Such behavior has recently been investigated on the microscopic where a reorientation of ellipsoidal latex particles is seen at an air-water interface in response to an increase in the surface pressure. However, when size of the objects approach the nanoscopic level, the theoretical arguments suggest that line tension becomes important. We discuss the self-assembly of tri-*n*-octylphosphine oxide (TOPO)-covered cadmium selenide (CdSe) nanorods at the oil (toluene or chloroform)/water interfaces. The packing of the nanorods on the droplets was studied by small angle neutron scattering (SANS). It was found that, as a nanorod-covered droplet was allowed to evaporate, an in-plane compression developed due to the decrease in the surface area which caused the nanorods to exhibit a range of two-dimensional structures that spanned across the phase diagram predicted theoretically.

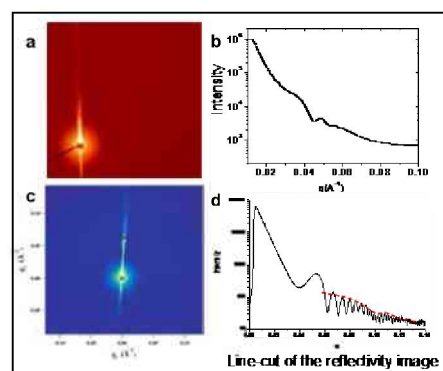
The packing of the nanorods (~8nm in diameter, ~30 nm in length) at the interface of water droplets suspended in the oil was studied by transmission SANS. The neutron scattering length densities of H₂O and D₂O are $-0.56 \times 10^{10} \text{ cm}^{-2}$ and $6.34 \times 10^{10} \text{ cm}^{-2}$, respectively. An H₂O/D₂O mixture with a 0.425 volume fraction of D₂O was used as the water phase to contrast match chloroform with a neutron scattering length density of $2.36 \times 10^{10} \text{ cm}^{-2}$. The nanorod-coated droplets were prepared as described in the experimental and loaded into a 2-mm thick sample cells. SANS measurements were conducted at room temperature for 12 hrs. The background corrected SANS profiles for the TOPO-covered CdSe nanorod assemblies shows a power law dependence of the form $I(q) \propto q^{-2.45 \pm 0.01}$ (blue line at low q) where q is related to the neutron wavelength λ and the scattering angle 2θ by $q = 4\pi \sin \theta / \lambda$. The average thickness t of the assembly of nanorods at the interface was found to be $6.3 \pm 0.3 \text{ nm}$ by a modified Guinier approximation for sheet-like objects. Since the average cross-sectional thickness of a rod is related to its radius, the observed thickness of these sheets, $t = 6.3 \pm 0.3 \text{ nm}$, is in good agreement with a sheet of rods with a radius of $4.0 \pm 0.2 \text{ nm}$. Any other type of orientation of the nanorods would results in a markedly greater layer thickness due to their anisotropic shape. No pronounced inter-particle correlations were seen which, more than likely, is due to the low coverage of nanorods on the droplet interfaces.

If nanorod-stabilized water droplets are dried on a carbon-coated copper grid, the in-plane packing of the nanorods was found to vary across the droplet showing a range of structures that spanned the complete phase diagram of nanorods, as predicted by Lekkerkerker and Frenkel. The transmission electron microscopy (TEM) image of one droplet is shown. At the periphery of the dried droplet, where the concentration of the nanorods was lowest, a smectic ordering of the nanorods oriented parallel to the surface is seen. The separation distance between two smectic layers and two nanorods is around 3~4nm. As the center of the dried droplet is approached, the concentration of the nanorods increases and a columnar phase is seen where the nanorods, oriented parallel to the surface, assemble end-to-end with a ~2 nm separation distance between two columns. At the center of the



dried droplet, a 2-D hexagonal array of nanorods oriented normal to the interface is seen. It should be emphasized that this process occurs in the absence of any external field.

Interfacial Behavior of Bionanoparticles: TMV is a rigid hollow cylinder of typical length 300 nm and diameter 18 nm. It has been confirmed by the *ex-situ* SFM results that the geometry of TMV at interfaces will be affected by the concentration in the bulk. At a low concentration in the bulk, TMV particles lie parallel at the interface, but at a high concentration, it orients normal to the interface. To capture the *in-situ* status of TMV at the interface, the SANS experiments were carried out at IPNS in Argonne national lab. As shown in the figure (a) at low concentration 0.2 mg/ml of TMV in the potassium phosphate buffer solution (0.01M, pH= 7.0), almost none signal was detected which is due to a very low surface coverage at the oil/water interface. As the concentration increased to 1mg/ml in 0.01M potassium phosphate buffer solution, a correlation peak was seen at $q_y = 0.0147\text{\AA}^{-1}$, which relates to an average separation distance of ~ 43 nm between the TMV nanoparticles. The power law dependence of the form $I(q) \propto q^{-2.25 \pm 0.17}$ indicates a monolayer of TMV at the

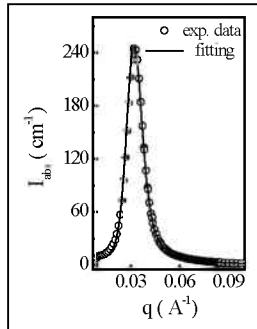


oil/water interface. As the concentration of the potassium phosphate buffer solution increased from 0.01M to 0.03M (pH=7), with the same concentration of TMV 1mg/ml in the solution, a power law dependence of the form $I(q) \propto q^{-1.89 \pm 0.07}$ with a correlation peak shifting to $q_y = 0.017\text{\AA}^{-1}$ was observed, which indicates that besides the concentration effect of TMV in the solution, changes of the ionic strength in the buffer solution can also affect the structures of TMV at the oil/water interface. To determine the orientation of the TMV at the oil/water interface, the SAXS experiments were carried out at the interfaces at ID-12 and ID-15 at advanced photon source at Argonne National Laboratory. A series of fringes indicating the layer thickness (~ 70 nm) at the interface was seen. After assembly at the interface for 16 hours, two sets of interference fringes were observed, indicating a double-layer structure ($\sim 150\text{nm}$ and ~ 15 nm) at the interface.

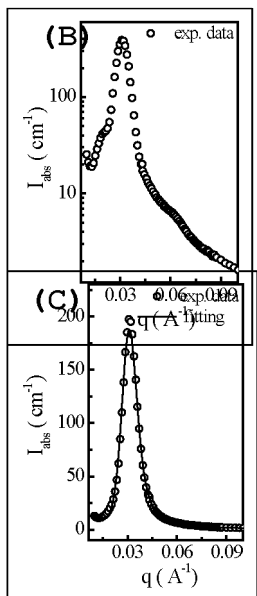
The Influence of Ion-Complexes on Phase Behavior of PS-*b*-PMMA Copolymers:

Polystyrene-*b*-poly(methyl methacrylate) (PS-*b*-PMMA) copolymers have been investigated in numerous laboratories for the generation of nanoporous templates in thin films through the control of the orientation of the microdomains by manipulating surface interactions [1] or by use of an external electric field [2]. However, due to the weak segmental interaction, obtaining films that show a long-range lateral order or templates with smaller pore sizes less than 10nm has been a challenge with PS-*b*-PMMA copolymers [3]. Moreover, because of the weak temperature dependence of χ ($\chi = (0.028 \pm 0.002) + (3.9 \pm 0.06)/T$) [4], the degree of microphase separation can only be realistically tuned by changing the degree of polymerization N, which is rather tedious. Recently, we found an increase of microdomain spacing and degree of ordering in a symmetric PS-*b*-PMMA copolymer as a consequence of the formation of lithium-PMMA

complexes via the coordination of lithium ions with carbonyl groups in PMMA [5, 6].



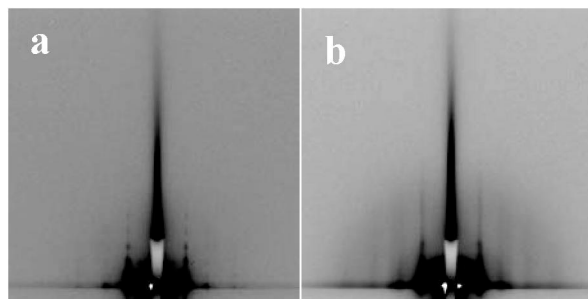
Furthermore, the formation of ionic complexes also induces a disorder-to-order transition for PS-*b*-PMMA copolymers having a low molecular weight and an order-to-order transition. These observations indicate that the segmental interaction parameter χ between PS and PMMA and the chain conformation may be modified by the formation of lithium-PMMA complexes. Small angle neutron scattering (SANS) is a very powerful means to study the phase behavior of block copolymers. Consequently, the parameters such as R_g and χ can be quantitatively obtained by analysis of the angular dependence of the SANS.



SANS profiles of a neat symmetric dPS-*b*-PMMA copolymer ($M_n = 28 \text{ kg/mol}$) and the copolymer with lithium-PMMA complexes. SANS profile for the neat copolymer exhibits a single, broad peak with a maximum at $q_{\text{max}} = 0.3284 \text{ nm}^{-1}$ and a full width at half maximum (FWHM) of 0.106 nm^{-1} (A), in agreement with previous studies [4]. This might indicate that the neat copolymer is in the phase-mixed state. Applying Leibler formalism to calculate the scattering profile gives a value of $\chi = 0.03686$ and a dPS statistical segment length of 8.77 \AA and a PMMA statistical segment length of 8.92 \AA . After $\sim 13.4 \%$ carbonyl groups are complexed with lithium ions, the reflection sharpens (FWHM of 0.097 nm^{-1}) and shifts to the left at $q_{\text{max}} = 0.3205 \text{ nm}^{-1}$ (B). For this sample, no good fitting of the scattering profile can be achieved by Leibler formalism, suggesting the copolymer is driven away from the phase-mixed state but not fully microphase-separated yet due to the absence of the higher ordered reflections. With increasing the addition of lithium ions and complexation (up to $\sim 25.3 \%$), the reflection continues to sharp (FWHM of 0.073 nm^{-1}) and shift to an even lower q ($q_{\text{max}} = 0.3129 \text{ nm}^{-1}$) together with a second order reflection (C), indicates that the copolymer is completely driven from a phase-mixed into a microphase separated state, i.e., a DOT occurs.

The Influence of Ion-Complexes on Phase Behavior of PS-*b*-PMMA Copolymers:

Our previous studies have shown that the addition of small amounts of salts, on the order a few ions per chain, induced significant enhancement of the ordering of the polystyrene-*b*-polyethyleneoxide (PS-*b*-PEO) copolymer films during solvent annealing and solvent evaporation. With the addition of certain amounts of salts, we observed that the copolymer microdomains remained ordered at a high degree of swelling and an extremely large amount of lateral spatial correlations of the cylindrical microdomains was found in the swollen state in the presence of benzene vapor, as observed by *in-situ* GISAXS¹. Most recently, *In-situ* GISAXS measurements during solvent annealing in the presence of various other



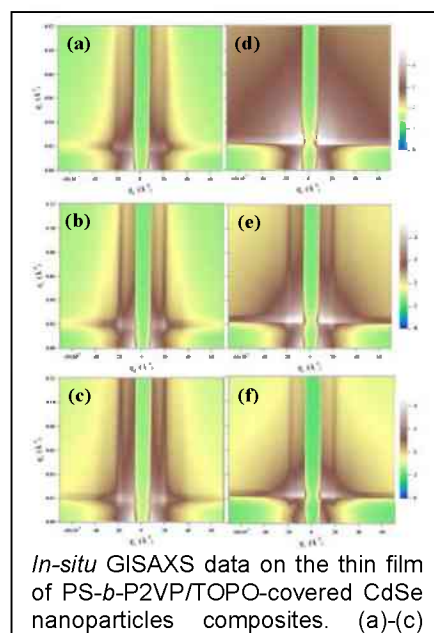
solvents (toluene, THF etc.) were carried out to further explore the ordering process. The change in the film thickness during swelling and upon removal of the solvent was measured simultaneously by multi-wavelength optical interferometry. For the PS-PEO sample with relatively higher salt concentration (molar ratio of $[O]/[K]=16$), as shown in the figure (rhs), the copolymer remains microphase separated throughout the swelling and many higher-order reflections are observed when film is swollen to 200% of the original thickness and further, indicating a very high degree of lateral ordering and correlation of the cylindrical microdomains. The Bragg rods (vertical streaks) in the GISAXS pattern can be attributed to the first order reflection from a 2D hexagonal lattice of cylinders of finite length oriented normal to the surface. It is interesting to note that the ordering behavior during swelling is independent of the solvent that was used for annealing. The increased non-favorable interactions, coupled with the enhanced mobility of the polymer chains in the highly swollen film, give rise to the exceptional degree of lateral ordering in the film seen in the GISAXS pattern.

References

- [1] Ryu D.Y.; Shin K.; Drockenmuller E.; Hawker C. J.; Russell T. P. *Science*, 2005, 308, 236.
- [2] Thurn-Albrecht T.; Schotter J.; Kästle G. A.; Emley N.; Shibauchi, T.; Krusin-Elbaum L.; Guarini K.; Black C. T.; Tuominen M. T.; Russell T. P. *Science*, 2000, 290, 2126.
- [3] Xu, T.; Kim, H-C.; DeRoche J.; Seney C.; Levesque C.; Martin P.; Stafford C. M.; Russell T. P. *Polymer*, 2001, 42, 9091.
- [4] Russell, T. P.; Jr., R. P. Hjelm; Seeger, P. A. *Macromolecules*, 1990, 23, 890.
- [5] Wang, J. Y.; Xu, T.; Leiston-Belanger, J.; Gupta, S.; Russell, T. P. *Phys. Rev. Lett.* 2006, 96, 128301.
- [6] Wang J. Y.; Leiston-Belanger J. M.; Sievert J. D.; Russell T. P. *Macromolecules*, 2006, 39, 8487.

Pickering Emulsions from Turnip Yellow Mosaic Virus Nanoparticles:

The self-assembly of monolayers of turnip yellow mosaic virus (TYMV) at the oil/water (O/W) interface was investigated using emulsions and planar interfaces. Robust monolayer assemblies of the TYMV were produced by cross-linking the interfacial assemblies. TYMV maintained its structure and integrity under different assembly conditions. The emulsion droplets were fully covered TYMV as evidenced by transmission electron microscopy (TEM) and scanning force microscopy (SFM). Tensiometry and small-angle neutron scattering (SANS) supported this finding. However, long-range ordering of the TYMV particles was not observed with the emulsions. Highly ordered, hexagonal arrangements of the TYMV, however, were



In-situ GISAXS data on the thin film of PS-*b*-P2VP/TOPO-covered CdSe nanoparticles composites. (a)-(c) Experimental data from *in-situ* GISAXS measurements below the critical angle (0.14°) during thermal annealing: (a) a freshly spin-coated thin film of the diblock copolymer and nanoparticles (0 hr); (b) annealed for 4 hrs; (c) annealed for 14 hrs. (d)-(f) Experimental data from GISAXS measurements above the critical angle (0.18°) during thermal annealing: (d) a freshly spin-coated thin film of the diblock copolymer and nanoparticles (0 hr); (e) thermally annealed for 4 hrs; (f) thermally annealed for 14 hrs.

found on planar O/W interfaces. The introduction of dehydroabietyl amine (DHAA) in the organic phase resulted in strong electrostatic interactions between the TYMV particles at the interface. pH and ionic strength of the buffer also could be used to enhance the lateral ordering of the TYMV assembled at the O/W interface. TEM and SFM showed clear evidence that these highly ordered TYMV assemblies could be stabilized by cross-linking.

Self-assembly of nanoparticle/copolymer mixtures: kinetics and universality:

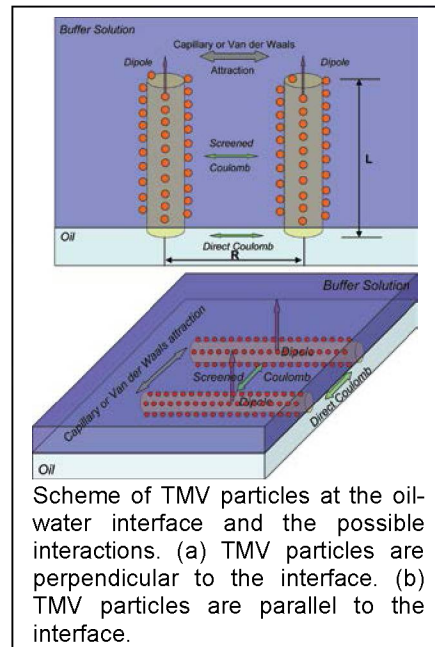
Designing novel hybrid materials provides a means of controlling electrical, magnetic or optical properties. There have been numerous studies on preparing nanocomposite materials. One approach is synthesizing inorganic nanoparticles within the microdomain of a well-ordered block copolymer template. In a second approach the self-assembled microdomain morphology of block copolymers is used to control the spatial arrangement of nanoscopic elements within the materials. The manipulation of the location of the nanoparticles in the materials can be achieved by controlling the sizes and the surface properties of the nanoparticles. Recent theoretical arguments suggest that synergistic interactions between self-organizing particles and a self-assembling matrix material may lead to hierarchically ordered structures. These predictions were recently confirmed in studies of a diblock copolymer having a cylindrical microdomains with added nanoparticles. In this study a co-operative, coupled interaction was found that led to hierarchically ordered structures upon thermal or solvent annealing where self-orienting, self-assembling arrays of microdomains were found without the use of external fields. However, the details of the structural evolution, and the means of manipulating the synergistic interactions, were not described, which is key for generalizing these concepts to different systems. To capture the detailed structural evolution of the self-assembly process in thin films of the nanoparticles/copolymer-mixtures, *in-situ* grazing incident small angle X-ray scattering (GISAXS) was used. We investigated the structural evolution in thin films of a polystyrene-*block*-poly(2-vinylpyridine) copolymer, denoted as PS-*b*-P2VP, mixed with tri-*n*-octylphosphine oxide-(TOPO)-covered cadmium selenide (CdSe) nanoparticles. Even with the strong interfacial interactions of P2VP with the substrate, the addition of the nanoparticles to the strongly microphase-separated copolymer is seen to modify interfacial interactions and cause the microdomains to orient normal to the surface. In conjunction with our previous studies, a universality of these synergistic interactions is suggested.

Self-assembly of Tobacco Mosaic Virus at Oil/Water Interfaces: The self-assembly of nanoscale objects into ordered structures has attracted significant attention for generating novel optical, electronic, and magnetic materials and devices. The use of liquid interfaces as platforms to assemble inorganic nanoparticles has been reported. Recently, bionanoparticles, like ferritin, cowpea mosaic virus (CPMV), tobacco mosaic virus (TMV), have also been of interest, due to their monodisperse size, the high-yield production of the virus particles and the versatile functionalities on the protein shell that can be modified by genetic or chemical modification.

Unlike spherically symmetric colloidal particles or nanoparticles, anisotropic nanoparticles show interesting structures and orientations at interfaces due to their shape. However, detailed information on the influence of concentration, ionic strength,

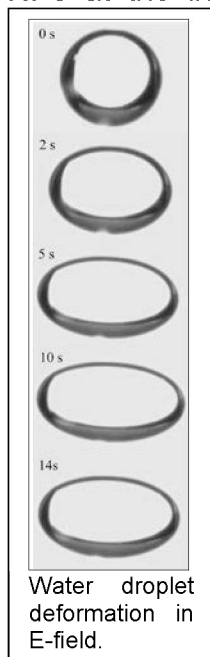
pH and aspect ratio of the particle on the characteristics of the assemblies of the protein nanoparticles at the interface is still unknown, but such information is essential for designing hierarchically ordered structures. Anisotropic rod-like TMV has a single characteristic diameter which is ideal for studying the self-assembly and ordering of these rod-like particles. We systemically studied the assembly of TMV at liquid-liquid interfaces as a function of TMV concentration and the ionic strength, and pH of the solution.

The self-assembly of tobacco mosaic virus (TMV) at oil/water interfaces has been studied *in situ* by tensiometry, small-angle x-ray and neutron scattering (SAXS and SANS). TMV showed different orientations at the perfluorodecalin/water interface as the concentration was changed in the bulk. At low concentrations of TMV in the aqueous phase, TMV assembled parallel to the interface with a random in-plane orientation so as to mediate the interfacial interactions. At high concentrations, TMV oriented normal to the interfaces, not only mediating the interfacial interactions but also neutralizing the strong electrostatic repulsion between the TMVs. We found that the repulsive forces between TMVs dominated the in plane packing, which was strongly affected by the ionic strength and the bulk solution, but not by the pH in the range of pH = 6-8.



Scheme of TMV particles at the oil-water interface and the possible interactions. (a) TMV particles are perpendicular to the interface. (b) TMV particles are parallel to the interface.

Dynamics of liquid/liquid interfacial jamming: Interfacial tension measurements indicated that the self-assembly of NPs at fluid interfaces occurs in three stages: NP diffusion to the interface, adsorption of NPs at the interface, and lateral packing of the NPs at the interface. The dynamics of each stage are different, and understanding these dynamics is major focus of the proposed studies. Studies performed to understand the equilibrium interfacial dynamics of different concentrations of NPs showed that systems with different nanoparticle concentrations reached different equilibrium states. These data indicate that measuring the non-equilibrium state by varying NP concentration is possible.



Water droplet deformation in E-field.

CdSe nanoparticles (3.4 nm radius) were dispersed in toluene and absorbed to the water/toluene interface. Relaxation time scales ranged from 0.5-100 s with changing NP concentration. $g_2(t)$ for systems with different NP concentrations were determined. The compression coefficient γ was found to change from 0.5 to 1.5, indicating a change from Brownian dynamics to hyperdynamics with increasing NP concentration. The relaxation time obeyed a power law of $\tau \approx q^{-n}$ with n changing from 2 to 1, reflecting the change in dynamics. This change in the dynamics reflects a change from an unjammed to jammed state.

Stabilizing Liquid Drops of Arbitrary Shape by the Interfacial

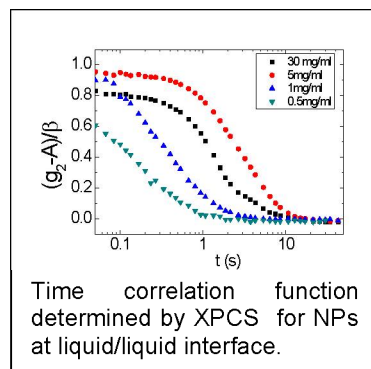
Jamming of Nanoparticles: Nanoparticles, NPs, assemble at the interface between two fluids into disordered, liquid-like arrays where the NPs can diffuse laterally at the interface. By changing the shape of the liquid domain with an external field, the surface area increases, and more NPs adsorb to the interface; by releasing the field, the drive to decrease interfacial area jams the NPs, arresting further shape change. Unlike the case of colloids-stabilized droplets, the jammed NPs remain liquid-like, enabling multiple, consecutive deformation and jamming events. The inherently weak force that limits the interfacial assembly of NPs is overcome by generating nanoparticle-surfactants *in situ*. Further stabilization is realized when di-functional additives are used for crosslinking the assemblies. The ability to generate and stabilize liquids with a prescribed shape poses unique opportunities for reactive liquid systems, storage and delivery.

Dynamics of polymer-nanoparticle hybrid materials: We used XPCS to study the dynamics of polymer-gold NP hybrid materials on length scales from tens of nanometers to microns. Dynamic information was derived from an autocorrelation:

$$g^{(2)}(q,t) = \langle I(t)I(t+\tau) \rangle = A + \beta e^{-2(t/\tau)^\gamma} \quad \tau \approx q^{-n}$$

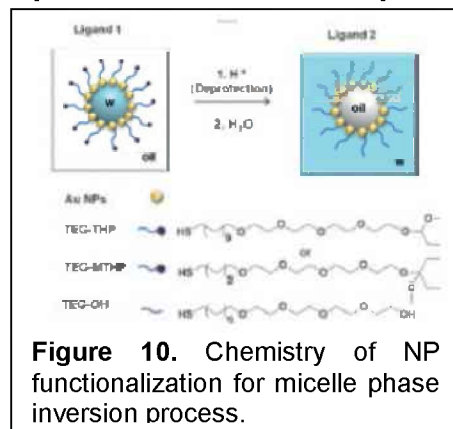
where A is the baseline, β is the contrast, τ is the relaxation time, and γ is the compression coefficient, dependent on the shape of relaxation.

Gold nanoparticles (NPs) (16 or 35 nm in diameter) functionalized with thiol-terminated polystyrene (PS) were dispersed in a PS matrix (Mw=10-24 kg/mol) at a 0.5 volume percent. The temperature was varied from $T_g+10^\circ\text{C}$ to $T_g+50^\circ\text{C}$. XPCS experiments were performed on sector 8-ID of the Advanced Photon Source using 7.35 keV x rays. $g_2(t)$ for PS 10k with 18 nm gold nanoparticles stabilized with 18 k g/mol polystyrene ligands at 120, 135 and 150 °C. τ was found to decrease with increasing T and with increasing q, such that $\tau \sim q^{-n}$, with $n=1$. This indicates that the diffusion of the NPs follows hyperdiffusive dynamics, where the relaxation time decreases with decreasing length scale.



Triggered 'in situ' Disruption and Inversion of Nanoparticle Stabilized Droplets:

Gold NPs and CdSe quantum dots that change wettability in the presence of acid (H^+) were prepared by nanoparticle surface functionalization with pyran-containing ligands that undergo facile de-protection and convert the NPs from hydrophobic to hydrophilic. These ligand-tailored nanoparticles were utilized to prepare water-in-oil (w/o) emulsions that were disrupted, and inverted, *in-situ*, to oil-in-water (o/w) systems simply by lowering the pH and adjusting the o/w ratio. The inversion process was also triggered by light, when a photo-acid generator (PAG) was present. The rate of emulsion disruption was sensitive



to the pyran substitution pattern, with a methoxy-substituted version giving a more rapid response to external stimuli.

Assembly of Graphene Oxide at Water/Oil Interfaces: Tessellated Nanotiles: The interfacial assembly of graphene oxide (GO) at the water/oil interface and its kinetics were systematically studied. GO nanosheets were found to segregate to the water/oil interface, and interact with quaternized block copolymers chains by the peripheral carboxyl groups on the GO. If the interfacial area is decreased, the interfacially confined GO jams, then buckles. An analysis of the kinetics of the assembly processes leads to the conclusion that diffusion of GO to the interface is the rate-determining step. The morphology of the jammed GO film was investigated and TEM image shows that GO sheets form a mosaic or a tiling at the oil/water interface.

Interfacial Activity of Acid-functionalized Single-walled Carbon Nanotubes at Water/Oil Interfaces: A novel route to segregate SWCNT-COOH at the interface between two immiscible fluids was developed by interacting with PS-NH₂ that dissolved in the oil phase through ammonium salt formation. The nature of the end-group and the molecular weight of the polystyrene significantly influence the interfacial assembly of the CNTs at the interface. A sharp transition in the interfacial tension was observed with concentration of CNTs that can be attributed to multiple PS functionalizations on the GO surface. By changing the pH with the concentration of the SWCNT solution, the pKa was changed, markedly altering the interaction of the acid groups on the SWCNT with the amine functionality on the PS. A randomly paced arrangement of SWCNTs at the interface was observed, suggesting that, once at the interface, the SWCNTs interact with the PS and are kinetically trapped in place.

Personnel Supported:

Graduate Research Students

1. Gajin Jeong
2. Xuan Ding
3. Mengmeng Cui
4. Kathleen McEnnis
5. Caroline Miesch
6. Wei Zhao
7. Xinyu Wei
8. Brenton Hammer
9. Yunxia Hu
10. Le Li
11. Xiaodan Gu
12. Weiyin Gu
13. Ravisubhash Tangirala
14. Qingling Zhang
15. Wei Chen
16. Jiayu Wang

17. Sivakumar Nagarajan
18. Dian Chen
19. Narupol Intasanta
20. Kan Du
21. Elizabeth Glogowski
22. Jinbo He
23. Ling Yang

Post Doctoral Fellows

1. Sung Woo Hong
2. Haeng-Deog Koh